

Tighter Confidence Intervals for Rating Systems

Robert Nowak, Ervin Tanczos

December 10, 2019

Abstract

Rating systems are ubiquitous, with applications ranging from product recommendation to teaching evaluations. Confidence intervals for functionals of rating data such as empirical means or quantiles are critical to decision-making in various applications including recommendation/ranking algorithms. Confidence intervals derived from standard Hoeffding and Bernstein bounds can be quite loose, especially in small sample regimes, since these bounds do not exploit the geometric structure of the probability simplex. We propose a new approach to deriving confidence intervals that are tailored to the geometry associated with multi-star/value rating systems using a combination of techniques from information theory, including Kullback-Leibler, Sanov, and Csiszar inequalities. The new confidence intervals are almost always as good or better than all standard methods and are significantly tighter in many situations. The standard bounds can require several times more samples than our new bounds to achieve specified confidence interval widths.

1 Introduction

Multi-star/value rating systems are ubiquitous. Ratings are used extensively in applications ranging from recommender systems [1, 11] to contests [19] to teaching evaluations [6, 5]. Key decisions are made based on comparing functionals of rating histograms such as means and quantiles. Algorithms for ranking, multi-armed bandits, preference learning, and A/B testing rely crucially on confidence intervals for these functionals. This paper develops new constructions for confidence intervals for multistar rating systems that are often considerably tighter than most of the known and commonly used constructions, including Hoeffding, Bernstein, and Bernoulli-KL bounds. These are reviewed in Section 2.1.

Our main approach begins by considering the construction of confidence sets in the probability simplex based on finite-sample versions of Sanov’s inequality [7] or polytopes formed by intersecting confidence intervals for the marginal probabilities. With large probability, these sets include all probability mass functions that could have generated an observed set of ratings. An important aspect of these sets is that they automatically capture to the intrinsic variability of the ratings. For instance, if all of the ratings are 3 out of 5 stars, then the set is tightly packed in a corner of the simplex and is effectively much smaller than if the ratings were uniformly distributed over 1 to 5 stars. The simplex confidence sets can then be constrained based on the sort of functional under consideration (e.g., mean or median). These constraints take the form of convex sets in the simplex. Csiszar inequality [8] provides a refinement of Sanov’s bound for such convex sets.

We illustrate how these regions look in the 3-dimensional simplex in Figure 1. Finding the maximum and minimum values for the functional of interest within the intersection of the Sanov and Csiszar confidence sets yields a new confidence interval for multistar ratings that is sharper than all common constructions in almost all cases. Moreover, the new intervals can be easily computed via optimization, as discussed in Section 4. A representative example from a 5-star rating application (details in next section) is shown in Figure 2. The empirical Bernstein (blue) and Bernoulli-KL (red) bounds are the best existing bounds, but the former performs poorly in low sample regimes and the latter performs poorly in large sample regimes. The new bounds (orange and purple) perform uniformly best over all sample sizes.

1.1 Motivating Examples

Confidence intervals for ratings are used in ranking applications like the Cartoon Collections Caption Contest¹. Each week, contestants submit funny captions for a given cartoon image. Thousands of captions

¹www.cartooncollections.com

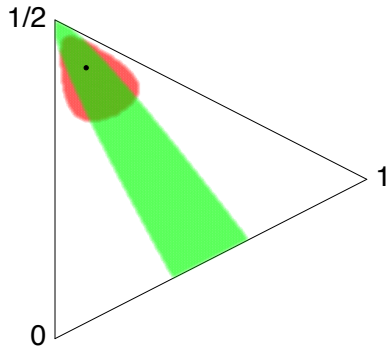


Figure 1: Confidence sets based on Sanov (red) and Csiszár (green) inequalities. Black dot is the empirical distribution in this case. The intersection is the set of distributions that may have generated the data.

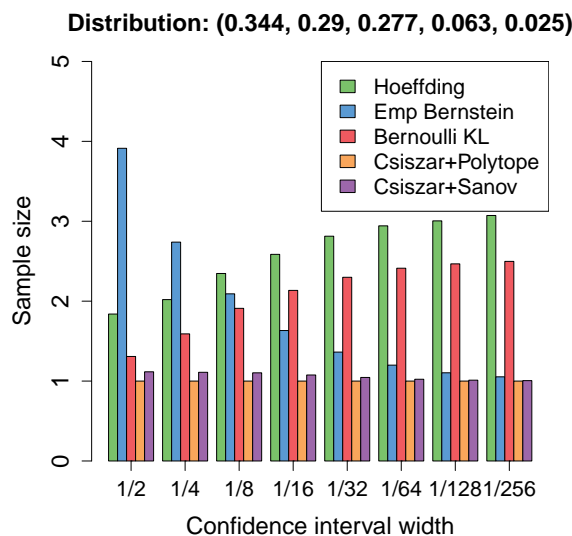


Figure 2: Comparison of sample sizes for specified confidence interval widths using different bounds. The 1 to 5 star distribution (.344, 0.29, 0.277, 0.063, 0.025) comes from a real-world contest rating dataset. The sample sizes are normalized relative to the best, so the new bounds (best) shown in orange and purple bars are height ≈ 1 . The empirical Bernstein bound (blue) requires about 4 times more samples than our new bounds in the small sample (large interval width) regime. The Bernoulli-KL bound (red) requires almost 3 times more samples in the large sample regime.

are submitted, and Cartoon Collections uses crowdsourcing to obtain hundreds of thousands of ratings for the submissions. Captions are rated on a 5-star scale and ranked according to the average rating each receives. The crowdsourcing system uses multi-armed bandit algorithms based on confidence intervals to adaptively focus the rating process toward the funniest captions, yielding a highly accurate ranking of the top captions. Better confidence intervals, like the Bernoulli-KL bound, can significantly improve the accuracy of the ranking, as demonstrated in [19]. The new confidence intervals developed in this paper offer even greater potential for improvements. For example, in a recent contest² one caption had the following histogram of 1 to 5 star ratings (365, 308, 294, 67, 27). This distribution is quite typical in this application. We use this distribution to simulate the rating process at different sample sizes. Figure 2 examines the (normalized) sample sizes required to achieve confidence intervals of various widths based on the different bounds. In general, the number of samples required for an interval of width W scales roughly like W^{-2} , and so we compare the relative number of samples needed by the different methods. The new bounds developed in this paper, called Csiszár-Polytope and Csiszár-Sanov, perform best over all sample sizes and require 2-4 times fewer ratings than standard bounds in many cases.

²Data courtesy of Cartoon Collections.

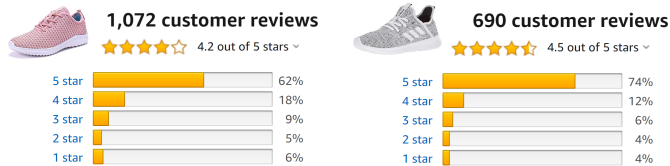


Figure 3: Two shoes with Amazon ratings.

As a second example, consider the two shoes and Amazon ratings shown in Figure 3. The shoe with fewer total ratings has a slightly higher average rating. Is the difference in average ratings statistically significant? To decide, we need to construct confidence intervals for the means based on the observed ratings. If the confidence intervals overlap, then the difference is not statistically significant. Our desired level of confidence will be expressed as $1 - \delta$, and for the purposes of this example we set $\delta = 0.1$.

The simplest type of bound is the Hoeffding bound. This results in confidence intervals of $[4.10, 4.40]$ and $[4.29, 4.67]$, respectively. The Bernoulli-KL bound [10] provides sharper bounds and yields the intervals $[4.13, 4.36]$ and $[4.34, 4.60]$, respectively. So we can not clearly conclude that Shoe 2 is better than Shoe 1. In fact, if the observed rating distributions were the true ones, and assuming equal samples for both shoes, we would require roughly 1250 samples per shoe using the Bernoulli-KL bound. Another option is to employ empirical Bernstein bounds [14], leading to intervals $[4.12, 4.38]$ and $[4.32, 4.63]$. Again, we can't decide which shoe is better. To do so would require roughly 1400 samples per shoe. However, our new bounds provide the intervals $[4.14, 4.35]$ and $[4.36, 4.59]$, allowing us to conclude that with probability at least 0.90 the true mean rating for Shoe 2 is larger. In this case, were the observed rating distributions true, confidence interval separation would occur at about 900 samples per shoe. So in order to determine that Shoe 2 is statistically better, the Bernoulli-KL and empirical Bernstein bounds require about 40% and 55% more ratings than our new bounds. In extensive experiments in Section 4, we demonstrate that all the standard bounds can require many times more samples than our new bounds to achieve specified confidence interval widths.

1.2 Related Work

Since multistar ratings are bounded, standard Hoeffding bounds can be used to derive confidence intervals. These bounds do not account for the bounded and discrete nature of multistar ratings, nor do they adapt to the intrinsic variance of ratings. Empirical versions of Bernstein's inequality [15, 14, 16, 2, 3] can be used to automatically adapt to the variance of the empirical process, but as we show these bounds are extremely loose in small sample regimes. For binary-valued (two-star) ratings, the best known bounds are based on the Kullback-Leibler (KL) divergence [10]. Bernoulli-KL bounds automatically adapt to the variance of binary processes and provide significantly tighter confidence bounds than standard Hoeffding or Bernstein bounds. All these bounds are reviewed in Section 2.1.

The Bernoulli-KL bound can be applied to bounded ratings by mapping the range into $[0, 1]$. These bounds have been shown theoretically and empirically significantly improve the performance of multi-armed bandit algorithms [19]. However, KL bounds are not well suited to general multistar rating processes and we show that our new bounds can provide significant improvements over naive reductions to the Bernoulli KL-type bounds. Confidence intervals for quantiles are used in many applications. For example, [18] considered quantile-based multi-armed bandit algorithms and used the Dvoretzky-Kiefer-Wolfowitz inequality to derive quantile confidence intervals. We show that for quantiles other than the median, our new bounds can yield tighter intervals.

The paper is organized as follows. We set up the problem and review existing results in Section 2. We define our proposed confidence bounds tailored for multistar random variables in Section 3, and analyze their accuracy and asymptotic performance. We also take a moment to review existing methods for inference about quantiles, given the similarities between those and the method we propose. Methods for computing the new confidence intervals and performance comparisons with other confidence intervals are the focus of Section 4. We provide concluding remarks in Section 5.

2 Problem setup

Let $\Delta_k := \{p_1, \dots, p_k : p_i > 0 \forall i, \sum p_i = 1\}$ denote the probability simplex in k -dimensions. Let $\mathcal{F} : \Delta_k \rightarrow [0, 1]$ be a bounded linear functional mapping from the probability simplex to $[0, 1]$ ³. The main focus of this work is to obtain tight confidence bounds for the value $\mathcal{F}(\mathbb{P})$, $\mathbb{P} \in \Delta_k$, based on an i.i.d. sample $X_1, \dots, X_n \sim \mathbb{P}$. We denote the empirical distribution based on n i.i.d. samples by $\hat{\mathbb{P}}_n$.

If \mathcal{F} is linear then $\mathcal{F}(\mathbb{P}) = \sum_{i \in [k]} p_i w_i$ for any $\mathbb{P} \in \Delta_k$, where $w_i \in \mathbb{R}$ are given weights and $[k]$ denotes the set $\{1, \dots, k\}$. Furthermore we can assume w.l.o.g. that $\mathcal{F} = \sum_{i \in [k]} w_i p_i$ with $w_1 = 0$ and $w_k = 1$. Thus the problem of estimating the value of a linear functional $\mathcal{F}(\mathbb{P})$ is equivalent to estimating the mean of the random variable ξ defined as $\mathbb{P}(\xi = w_i) = p_i$. In the discussions that follow, it will be useful to keep both interpretations of the problem in mind. Finally, we will also consider cases when $\mathcal{F}(\mathbb{P})$ is a quantile, due to its practical relevance and its similarity to linear functionals.

2.1 Contributions

The most commonly used concentration bounds for the mean of variables bounded in $[0, 1]$ are Hoeffding's inequality, Bernstein's inequality and the Bernoulli-KL bound (see equation (4) below and [4] for details). The key difference between these bounds is the variance information they use. It is straightforward to see that for a random variable $X \in [0, 1]$, the variance can be upper bounded as follows

$$\text{Var}(X) = \mathbb{E}(X^2) - \mathbb{E}^2(X) \leq \mathbb{E}(X)(1 - \mathbb{E}(X)) .$$

The Bernoulli-KL bound essentially uses the upper bound above, whereas Hoeffding's inequality further upper bounds the right hand side of the display above by $1/4$. Hence the Bernoulli-KL bound will always be stronger than Hoeffding's bound. However, the variance of X can be smaller than the bound above and Bernstein's inequality explicitly uses this variance information. Therefore it will be tighter than the Binary-KL bound when the variance is indeed smaller.

However, in practice one does not know the variance, and instead has to estimate it from the sample. This gives rise to the empirical Bernstein inequality [14], which states that with probability $\geq 1 - \delta$

$$\bar{X}_n - \mathbb{E}(X) \leq \sqrt{\frac{2 \text{Var}_n(X) \log(2/\delta)}{n}} + \frac{7 \log(2/\delta)}{3(n-1)} , \quad (1)$$

where \bar{X}_n is the empirical mean and $\text{Var}_n(X)$ is the empirical variance. Asymptotically, the inequality roughly says

$$\bar{X}_n - \mathbb{E}(X) \leq \sqrt{\frac{2 \text{Var}(X) \log(2/\delta)}{n}} ,$$

or in other words

$$\mathbb{P}(\bar{X}_n - \mathbb{E}(X) > \epsilon) \leq \exp\left(-n \frac{2\epsilon^2}{\text{Var}(X)}\right) . \quad (2)$$

This is the best exponent we can hope for in the limit, since the Central Limit Theorem results in the same exponent in the limit as $n \rightarrow \infty$.

Although (1) has good asymptotic performance, its small sample performance is poor. For small n the second term dominates the right hand side of (1), with the bound often becoming larger than 1, making the inequality vacuous. This property is often undesirable in practice, for instance in the context of bandit algorithms this can lead to wasting a large amount of samples on sub-optimal choices in the early stages of the algorithm. To overcome this drawback, we propose a confidence bound building on the works [17] and [8]. Using their results we construct a confidence region in the probability simplex that contains the true distribution \mathbb{P} with high-probability. Being specialized for distributions on k -letter alphabets, these bounds automatically adapt to both the variance and the geometry of the probability simplex. Taking the extreme values of the means of distributions within the confidence region yield the desired confidence bounds for the mean.

³We can rescale any bounded functional to the interval $[0, 1]$.

3 Results

In this section we present possible ways of constructing confidence sets in Δ_k for an unknown distribution \mathbb{P} based on the empirical distribution $\widehat{\mathbb{P}}_n$. For each method we review the information-theoretic inequality used and describe in detail how it leads to a confidence set in the simplex Δ_k . The confidence sets presented in Sections 3.1 and 3.2 are not designed with any specific functional in mind. In Section 3.3 we tailor these regions to specifically work well when \mathcal{F} is linear. Finally, we also briefly mention the case when \mathcal{F} is a quantile, and how it relates to the case of linear functionals in Section 3.4.

3.1 The Sanov-ball

Sanov's theorem [7] is a natural choice to construct a confidence region for \mathbb{P} .

Theorem 1 (Theorem 11.4.1 of [7]). *Let E be any subset of the probability simplex Δ_k . Then*

$$\mathbb{P}(\widehat{\mathbb{P}}_n \in E) \leq \binom{n+k-1}{k-1} \exp\left(-n \inf_{\mathbb{Q} \in E} \text{KL}(\mathbb{Q}, \mathbb{P})\right).$$

We can re-write this result as

$$\mathbb{P}\left(\text{KL}(\widehat{\mathbb{P}}_n, \mathbb{P}) > z\right) \leq \binom{n+k-1}{k-1} e^{-nz},$$

which leads to the confidence region

$$\left\{ \mathbb{Q} : \text{KL}(\widehat{\mathbb{P}}, \mathbb{Q}) \leq \frac{\log\left(\binom{n+k-1}{k-1}/\delta\right)}{n} \right\}.$$

Next, consider an improvement of Sanov's Theorem.

Theorem 2. [12] *For all k, n*

$$\begin{aligned} & \mathbb{P}\left(\text{KL}(\widehat{\mathbb{P}}_n, \mathbb{P}) > z\right) \\ & \leq \min \left\{ \frac{6e}{\pi^{3/2}} \left(1 + \sum_{i=1}^{k-2} \left(\sqrt{\frac{e^3 n}{2\pi i}}\right)^i\right) e^{-nz}, \right. \\ & \quad \left. 2(k-1)e^{-nz/(k-1)} \right\} \end{aligned}$$

Generally speaking, the first term in the bound is smaller than the second ⁴ when the sample size n is on the same order or lower than the alphabet size k . Since in this work we are primarily concerned with situations when the alphabet size is relatively small, we use the second term in the inequality above. This leads to the confidence region

$$\mathcal{C}_{\text{Sanov}} := \left\{ \mathbb{Q} : \text{KL}(\widehat{\mathbb{P}}, \mathbb{Q}) \leq \frac{(k-1) \log\left(\frac{2(k-1)}{\delta}\right)}{n} \right\}. \quad (3)$$

Roughly speaking, this improves a $\log n$ factor to a $\log k$ factor in the cutoff threshold, compared to the one we would get using Theorem 1.

⁴In particular, it can be shown that the second term is better whenever $k \leq \sqrt[3]{\frac{e^3}{8\pi}n}$, see [12].

3.2 Confidence Polytope

Another simple approach is to construct confidence bounds for the marginal probabilities p_j , $j \in [k]$ and combine them with a union bound. For each j let \hat{p}_j denote the empirical frequency of j . Since $n\hat{p}_j$ is the sum of independent $\text{Ber}(p_i)$ samples, we can use the Bernoulli-KL inequality [10]

$$\mathbb{P}(\text{KL}(\hat{p}_j, p_j) > z) \leq 2 \exp(-nz) . \quad (4)$$

This leads to the confidence-polytope

$$\mathcal{C}_{\text{Polytope}} := \left\{ \mathbb{Q} : \text{KL}(\hat{p}_j, q_j) \leq \frac{\log(2k/\delta)}{n}, \forall j \in [k] \right\} . \quad (5)$$

Note that it is not true in general that $\mathcal{C}_{\text{Sanov}}$ contains $\mathcal{C}_{\text{Polytope}}$ or vice-versa, and in fact most often neither one is contained in the other. For one, these sets have different geometries. Furthermore, the Bernoulli-KL inequality (and $\mathcal{C}_{\text{Polytope}}$ as a consequence) is essentially unimprovable, but there still might be room for improvement in (2) (see the discussion in [12]). Therefore, which confidence region performs better depends on the functional \mathcal{F} and the true distribution \mathbb{P} .

That being said, in all numerical experiments presented in Section 4 the bounds derived from $\mathcal{C}_{\text{Polytope}}$ consistently beat those derived from $\mathcal{C}_{\text{Sanov}}$.

3.3 Linear functionals

The main tool we use to construct confidence regions when \mathcal{F} is linear is Csiszár's theorem [8]⁵:

Theorem 3. *If E is a convex subset of the probability simplex, then*

$$\mathbb{P}(\hat{\mathbb{P}}_n \in E) \leq \exp\left(-n \inf_{\mathbb{Q} \in E} \text{KL}(\mathbb{Q}, \mathbb{P})\right) .$$

This theorem can be viewed as a sharpening of Sanov's theorem for convex sets, or as a generalization of the Bernoulli-KL inequality (as we illustrate in Proposition 2 below). Denote the level sets of the functional \mathcal{F} by

$$\mathcal{R}_m := \{\mathbb{Q} : \mathcal{F}(\mathbb{Q}) = m\} ,$$

and let

$$B(\mathbb{Q}, z) = \{\mathbb{Q}' : \text{KL}(\mathbb{Q}', \mathbb{Q}) < z\}$$

denote the KL-ball of radius z around distribution \mathbb{Q} . With this we can define the confidence region

$$\mathcal{C}_{\mathcal{F}}(\hat{\mathbb{P}}_n, z) = \left\{ \mathbb{Q} : \mathcal{R}_{\mathcal{F}(\hat{\mathbb{P}}_n)} \cap B(\mathbb{Q}, z) \neq \emptyset \right\} .$$

We have the following guarantee for this confidence region:

Proposition 1. *If $\hat{\mathbb{P}}_n$ is the empirical distribution of an i.i.d. sample coming from true distribution \mathbb{P} , then*

$$\mathbb{P}\left(\mathbb{P} \notin \mathcal{C}_{\mathcal{F}}(\hat{\mathbb{P}}_n, z)\right) \leq 2e^{-nz} .$$

Proof. By the definition, if $\mathbb{P} \notin \mathcal{C}_{\mathcal{F}}(\hat{\mathbb{P}}_n, z)$ implies that

$$\mathcal{R}_{\mathcal{F}(\hat{\mathbb{P}}_n)} \cap B(\mathbb{P}, z) = \emptyset .$$

This can be restated as

$$\mathcal{F}(\hat{\mathbb{P}}_n) \notin \left[\min_{\mathbb{Q} \in B(\mathbb{P}, z)} \mathcal{F}(\mathbb{Q}), \max_{\mathbb{Q} \in B(\mathbb{P}, z)} \mathcal{F}(\mathbb{Q}) \right] .$$

Using the notation $L = \min_{\mathbb{Q} \in B(\mathbb{P}, z)} \mathcal{F}(\mathbb{Q})$ and $U = \max_{\mathbb{Q} \in B(\mathbb{P}, z)} \mathcal{F}(\mathbb{Q})$ we have

$$\mathbb{P}(\mathbb{P} \notin \mathcal{C}_{\mathcal{F}}(\hat{\mathbb{P}}_n, z)) = \mathbb{P}\left(\hat{\mathbb{P}}_n \in \left(\bigcup_{z < L} \mathcal{R}_z\right) \cup \left(\bigcup_{z > U} \mathcal{R}_z\right)\right) .$$

Note that both regions $\bigcup_{z < L} \mathcal{R}_z$ and $\bigcup_{z > U} \mathcal{R}_z$ are convex, since they are unions of 'adjacent' hyperplanes. Using a union bound and Theorem 3 concludes the proof. \square

⁵For sake of completeness we include the proof of this theorem in the Supplementary Material.

According to this result

$$\mathcal{C}_{\mathcal{F}} := \mathcal{C}_{\mathcal{F}} \left(\widehat{\mathbb{P}}_n, \frac{\log(2/\delta)}{n} \right) \quad (6)$$

contains \mathbb{P} with probability $1 - \delta$. Note that $\mathcal{C}_{\mathcal{F}}$ is the KL “neighborhood” of the level set $\mathcal{R}_{\mathcal{F}(\widehat{\mathbb{P}}_n)}$. As the next result shows, this neighborhood is widest near the edge of the simplex connecting the corners $(1, 0, \dots, 0)$ and $(0, \dots, 0, 1)$ (also see Figure 4). This is under the assumption that the weights of \mathcal{F} are monotonically increasing (e.g., rating values of 1 to k stars).

Proposition 2. *Fix a $z > 0$ and any $\widehat{\mathbb{P}}_n$, and consider the set $\mathcal{C}_{\text{Linear}}$. Define*

$$L = \min_{\mathbb{Q} \in \mathcal{C}_{\mathcal{F}}} \mathcal{F}(\mathbb{Q}) \quad \text{and} \quad U = \max_{\mathbb{Q} \in \mathcal{C}_{\mathcal{F}}} \mathcal{F}(\mathbb{Q}) .$$

For any $\xi \in [0, 1]$ consider the distributions $\mathbb{P}_{\xi} = (1 - \xi, 0, \dots, 0, \xi)$ that take value $w_1 = 0$ with probability $1 - \xi$ and value $w_k = 1$ with probability ξ . Then the extreme values L and U are uniquely attained by the distributions \mathbb{P}_L and \mathbb{P}_U .

Proof. The proof for L and U are similar, so in what follows we focus on U . The claim is a simple consequence of the log-sum inequality. Specifically, consider any two distributions \mathbb{P} and \mathbb{Q} . We have

$$\begin{aligned} & \text{KL}(\mathcal{F}(\mathbb{P}), \mathcal{F}(\mathbb{Q})) \\ &= \left(\sum_{j \in [k]} w_j p_j \right) \log \frac{\sum_{j \in [k]} w_j p_j}{\sum_{j \in [k]} w_j q_j} \\ &+ \underbrace{\left(1 - \sum_{j \in [k]} w_j p_j \right)}_{= \sum_{j \in [k]} (1 - w_j) p_j} \log \frac{1 - \sum_{j \in [k]} w_j p_j}{1 - \sum_{j \in [k]} w_j q_j} \\ &\leq \sum_{j \in [k]} w_j p_j \log \frac{p_j}{q_j} + \sum_{j \in [k]} (1 - w_j) p_j \log \frac{p_j}{q_j} \\ &= \text{KL}(\mathbb{P}, \mathbb{Q}) , \end{aligned}$$

by applying the log-sum inequality for both terms on the right side of the first line separately. The inequalities are only tight when $w_j p_j = w_j q_j$ and $(1 - w_j) p_j = (1 - w_j) q_j \forall j \in [k]$ respectively. This can only happen if $\mathbb{P} \equiv \mathbb{Q}$. Using this inequality with any $\mathbb{P} \in \mathcal{R}_{\mathcal{F}(\widehat{\mathbb{P}}_n)}$ and any $\mathbb{Q} \in \mathcal{R}_U$ implies that the intersection between $\mathcal{C}_{\mathcal{F}}$ and \mathcal{R}_U is the single point \mathbb{P}_U , and the claim is proved. \square

Proposition 2 shows in exactly what sense Theorem 3 is a generalization of (4): the confidence bounds derived for $\mathcal{F}(\mathbb{P})$ using $\mathcal{C}_{\mathcal{F}}$ are the same as applying (4) to the bounded random variable ξ defined as $\mathbb{P}(\xi = w_i) = p_i$. However, Proposition 2 also shows that incorporating information about where $\widehat{\mathbb{P}}_n$ lies within the simplex might lead to smaller confidence regions, since $\mathcal{C}_{\mathcal{F}}$ is widest near the edge of the simplex connecting the corners $(1, 0, \dots, 0)$ and $(0, \dots, 0, 1)$, but is potentially narrower elsewhere. A natural way to do this is by intersecting $\mathcal{C}_{\mathcal{F}}$ with either $\mathcal{C}_{\text{Sanov}}$ or $\mathcal{C}_{\text{Polytope}}$. We denote the intersected regions by $\mathcal{C}_{\text{Csiszar+Sanov}}$ and $\mathcal{C}_{\text{Csiszar+Polytope}}$ respectively. Naturally, in order to maintain the same confidence level we need to combine the two regions using a union bound. We illustrate these regions in a 3-dimensional simplex in Figure 4.

3.3.1 Asymptotic performance

The proposition below shows that when we apply Theorem 3 in the context of linear functionals, the exponent in the bound is equal to what we would get from the central limit theorem. This shows that Theorem 3 is asymptotically tight. Based on this, we expect that the confidence bounds derived from both $\mathcal{C}_{\text{Csiszar+Sanov}}$ and $\mathcal{C}_{\text{Csiszar+Polytope}}$ have optimal asymptotic performance. In Section 4 we illustrate that these bounds enjoy very good performance across all sample sizes.

The full proof of the proposition below can be found in the Supplementary Materials. The high-level argument is that when ϵ is small, the minimizer of $\min_{\mathbb{Q} \in E} \text{KL}(\mathbb{Q}, \mathbb{P})$ will be close to \mathbb{P} . When \mathbb{P} and \mathbb{Q}

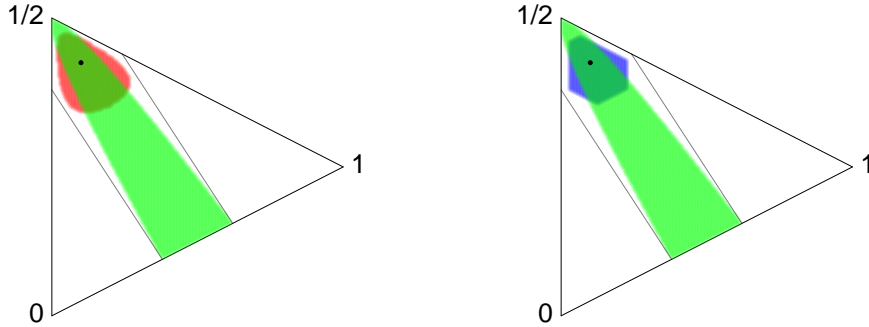


Figure 4: $\mathcal{C}_{\text{Csiszar+Sanov}}$ (left) and $\mathcal{C}_{\text{Csiszar+Polytope}}$ (right) for $\hat{\mathbb{P}}_n = (1/10, 8/10, 1/10)$, $n = 100$, $\delta = 0.05$, with $\mathcal{C}_{\mathcal{F}}$ indicated by the green region. The weights of the linear functional are $w_1 = 0, w_2 = 1/2, w_3 = 1$. The plots also include the level sets $\mathcal{R}_L, \mathcal{R}_U$ (black lines), where U and L are the values defined in Proposition 2. The plots illustrate how intersecting $\mathcal{C}_{\text{Sanov}}$ or $\mathcal{C}_{\text{Polytope}}$ with $\mathcal{C}_{\mathcal{F}}$ makes the former regions narrower in the direction perpendicular to $\mathcal{R}_{\mathcal{F}(\hat{\mathbb{P}}_n)}$ and improve the bounds as a result.

are close, $\text{KL}(\mathbb{Q}, \mathbb{P}) \approx \chi^2(\mathbb{Q}, \mathbb{P})$. Minimizing the chi-squared divergence instead of the KL-divergence on E would precisely give the value $\epsilon^2/(2 \text{Var}_{\mathbb{P}}(\mathcal{F}))$. The proposition shows that the exponent behaves like that of the Bernstein bound in equation (2).

Proposition 3. *Let $\mathcal{F}(\mathbb{P}) = \sum_{j \in [k]} w_j p_j$ be a linear functional. Let $\epsilon > 0$ and define $E = \{\mathbb{Q} : \mathcal{F}(\mathbb{Q}) > \mathcal{F}(\mathbb{P}) + \epsilon\}$. For ϵ small enough, the exponent in Theorem 3 can be bounded as*

$$\inf_{\mathbb{Q} \in E} \text{KL}(\mathbb{Q}, \mathbb{P}) \geq \frac{2\epsilon^2}{\text{Var}_{\mathbb{P}}(\mathcal{F})} - O(\epsilon^3),$$

where $\text{Var}_{\mathbb{P}}(\mathcal{F}) = \sum_{j \in [k]} w_j^2 p_j - (\sum_{j \in [k]} w_j p_j)^2$.

3.4 Quantiles

We now take a moment to review the problem of estimating quantiles of a discrete random variable.

The τ -quantile of a random variable X is defined as

$$\mathcal{Q}_{\tau}(X) = \inf\{x : \tau \leq F_X(x)\},$$

where $F_X(x) = \mathbb{P}(X \leq x)$ is the CDF. Without loss of generality we assume X takes values in $[k] = \{0, \frac{1}{k-1}, \dots, 1\}$ ⁶.

The standard method for constructing quantile confidence bounds is first constructing a confidence band for the CDF, and then taking the extreme values of the quantile among distributions in the CDF band. This approach fits the general strategy advocated in this work.

Perhaps the most well-known method to derive confidence bands for the CDF is the DKWM-inequality [13], which states

$$\mathbb{P}\left(\sup_x \left|\hat{F}_n(x) - F(x)\right| > z\right) \leq 2 \exp(-2nz^2),$$

where \hat{F}_n is the empirical CDF based on n samples. This method is widely used in practice, see for instance [18].

However, there exist confidence bands for the CDF that are uniformly better than those derived from the DKWM inequality, see [9] and references therein. In the context of discrete random variables taking finitely many values (e.g., multistar ratings), the bounds of [9] are equivalent to applying the Bernoulli-KL confidence bound for each point of the CDF (i.e. each point in the set $\{0, \frac{1}{k-1}, \dots, \frac{k-2}{k-1}\}$), and combining them with a union-bound.

⁶For random variables X and Y such that $Y = f(X)$ then $\mathcal{Q}_{\tau}(Y) = f(\mathcal{Q}_{\tau}(X))$.

If the union-bound is performed naively with the confidence equally allocated among the $k - 1$ points, then the latter confidence band is inferior to the one obtained from the DKWM inequality for values x where $F_X(x) \approx 1/2$. However, this drawback can be mitigated by allocating the confidence in a data-driven way, as described and illustrated in Section 4.

4 Computational Methods and Experiments

4.1 Linear functionals

We demonstrate the performance of the method described in Section 3.3 by numerical experiments. We compute the average number of samples needed for the confidence bound for the mean of level $\delta = 0.05$ to reach a certain width, for various methods⁷ and true distributions. We performed experiments with $k = 3$ and $k = 5$ and in each case $w_i = (i - 1)/(k - 1)$, $i = 1, \dots, k$. We choose a number of true distributions from the simplex representative of key geometric positions: the midpoint of the probability simplex (the uniform distribution), and midpoints of lower dimensional faces.

Recall that in order to compute the confidence bounds outlined in Section 3 we need to solve optimizations $\min_{\mathbb{Q} \in \mathcal{C}(\hat{\mathbb{P}}_n)} \mathcal{F}(\mathbb{Q})$ and $\max_{\mathbb{Q} \in \mathcal{C}(\hat{\mathbb{P}}_n)} \mathcal{F}(\mathbb{Q})$, where \mathcal{F} is linear. Since the sets $\mathcal{C}_{\text{Sanov}}$ and $\mathcal{C}_{\text{Polytope}}$ are convex, solving these optimizations is straightforward. However, for $\mathcal{C}_{\text{Csiszar+Sanov}}$ and $\mathcal{C}_{\text{Csiszar+Polytope}}$ the feasible region is itself defined by an optimization, and so the optimizations above become bi-level problems. In particular, for the set $\mathcal{C}_{\text{Csiszar+Sanov}}$ we need to solve

$$\begin{aligned} \min / \max_{q_1, \dots, q_k} \quad & \sum_{i \in [k]} w_i q_i \quad \text{s.t.} \\ & q_i \geq 0 \forall i \in [k], \sum_{i \in [k]} q_i = 1, \\ & \text{KL}(\hat{\mathbb{P}}_n, \mathbb{Q}) \leq z, \\ & \min_{\mathbb{P}' \in \mathcal{R}_{\mathcal{F}(\hat{\mathbb{P}}_n)}} \text{KL}(\mathbb{P}', \mathbb{Q}) \leq z', \end{aligned}$$

where $z, z' \in \mathbb{R}_+$ are chosen such that both $\mathcal{C}_{\text{Sanov}}$ and $\mathcal{C}_{\mathcal{F}}$ have confidence $\delta/2$ (see (3) and (6)). The problem for $\mathcal{C}_{\text{Csiszar+Polytope}}$ is analogous.

We solve the problem above using a binary search. Let $u \in [0, 1]$ be a fixed value, and suppose we want to decide whether or not $\min_{\mathbb{Q} \in \mathcal{C}_{\text{Csiszar+Sanov}}} \mathcal{F}(\mathbb{Q}) \leq u$. Deciding this is equivalent to solving

$$\begin{aligned} \min_{\mathbb{P}', \mathbb{Q}} \quad & \text{KL}(\mathbb{P}', \mathbb{Q}) \quad \text{s.t.} \\ & q_i \geq 0 \forall i \in [k], \sum_{i \in [k]} q_i = 1, \\ & p'_i \geq 0 \forall i \in [k], \sum_{i \in [k]} p'_i = 1, \\ & \text{KL}(\hat{\mathbb{P}}_n, \mathbb{Q}) \leq z, \\ & \sum_{i \in [k]} w_i p'_i = \mathcal{F}(\hat{\mathbb{P}}_n), \\ & \sum_{i \in [k]} w_i q_i = u. \end{aligned}$$

This is a minimization of a convex function subject to convex constraints, so it can be easily solved with standard solvers. We can combine this with a binary search to find $\min_{\mathbb{Q} \in \mathcal{C}_{\text{Csiszar+Sanov}}} \mathcal{F}(\mathbb{Q})$. Finding the maximum is analogous. We implemented all the optimization problems using the R package CVXR.⁸ Code for the optimization is provided in the Supplementary Materials file code.txt.

⁷Confidence intervals are restricted to lie within $[0, 1]$.

⁸This implementation may not be the most efficient way of computing these confidence bounds. Finding the most efficient implementation is an important practical consideration.

The experiments tell a similar story regardless of the true distribution, therefore we only show a few representative examples in Figure 5 and present more in the Supplementary Material. In general, the number of samples required for an interval of width W scales roughly like W^{-2} , and so we compare the relative number of samples needed by the different methods. We see that our proposed method has the most favorable sample complexity in almost all cases. Empirical Bernstein bound starts as a clear loser, requiring 4-5 times more samples than our new bounds in the large interval width (small sample) regimes. However, it matches our new bounds in the small width (large sample) regimes. The Bernoulli-KL bound performs better in large width regimes, but can become loose in small width regimes. For example, for the distribution $(0, 0, 1/3, 1/3, 1/3)$ the Bernoulli-KL bound requires about 4 times more samples than the new bounds to achieve a width of $1/128$. If the distribution is concentrated on 3 stars, as is the case $(0, 0.05, 0.9, 0.05, 0)$, then the poor performance of the Bernoulli-KL bound is dramatic. Note that the Bernoulli-KL is best when the true distribution is in fact Bernoulli, as is the case $(1/2, 0, 0, 0, 1/2)$, but our new bounds are almost as good. The reason *Csiszar+Sanov* and *Csiszar+Polytope* slightly under perform in this special case is due to the union bound that arises when we combine $\mathcal{C}_{\mathcal{F}}$ with $\mathcal{C}_{\text{Sanov}}$ or $\mathcal{C}_{\text{Polytope}}$. This effect could be mitigated by a data-driven union-bound that allocates most of the confidence budget to $\mathcal{C}_{\mathcal{F}}$ when $\hat{\mathbb{P}}_n$ is near the edge of the simplex connecting $(1, 0, \dots, 0)$ and $(0, \dots, 0, 1)$.

4.2 Quantiles

In this section we compare the performance of CDF bands obtained from the DKWM and Bernoulli-KL inequalities. The width of these bands around the τ -quantile directly influences the derived confidence bounds for the quantile. One possible way of measuring the width is

$$\text{Width}_{\tau} = \sum_{i \in [k]} |\min\{U_i - \tau, \tau - L_i\}| \mathbf{1}\{L_i \leq \tau \leq U_i\},$$

where $[L_i, U_i]$ are the confidence bounds for $F_X(i)$, $i \in [k]$. In Figure 6 we plot the average sample size needed for Width_{τ} to reach a certain value with $\delta = 0.05$, for the uniform distribution with $k = 5$ and various values for τ . We use two versions of the Bernoulli-KL CDF bounds: one with a naive union bound and one with a data-driven union bound. The heuristic behind the data-driven union bound is to assign more confidence to points of the CDF where the CDF value is close to τ . We do this as follows. Define $c_i = (i - \hat{\tau} + 1)^2$, $i \in [k]$, and $c = \sum_{i \in [k]} 1/c_i$, where $\hat{\tau}$ is the τ -quantile of $\hat{\mathbb{P}}_n$. Then we allocate $\delta/(c \cdot c_i)$ confidence for the bound on $F_X(i)$, $i \in [k]$. We do not claim that this is the best possible method, but it yields good results empirically (see purple bars in Figure 6) and we stress that this approach does yield valid confidence intervals.

Figure 6 show that the adverse effects of the union bound can be mitigated by using a data-driven method. The Bernoulli-KL method fares almost as well as DKWM when $\tau = 0.5$. However, as τ gets farther away from 0.5, the benefit of using Bernoulli-KL becomes more and more pronounced. This should come as no surprise, since Bernoulli-KL bound is the tightest possible method for constructing a confidence bound for any fixed point of the CDF. Since the adverse effects of union bounding can become more pronounced for larger alphabets, we present numerical experiments for larger alphabets in the Supplementary Material.

5 Conclusion

In this work we illustrated the merit of using information-theoretic inequalities for constructing confidence bounds for functionals of multistar random variables. These bounds account for the geometry of the probability simplex, and as a result exhibit excellent performance across all sample sizes when compared to other popular bounds in the literature. Conventional bounds may need up several times more samples to reach the same confidence interval width as the bounds proposed in this work. Although outside the scope of this work, the general recipe presented here might prove fruitful for functionals other than linear, such as the variance or higher moments. Extending these methods to other functionals is a fruitful avenue for future research.

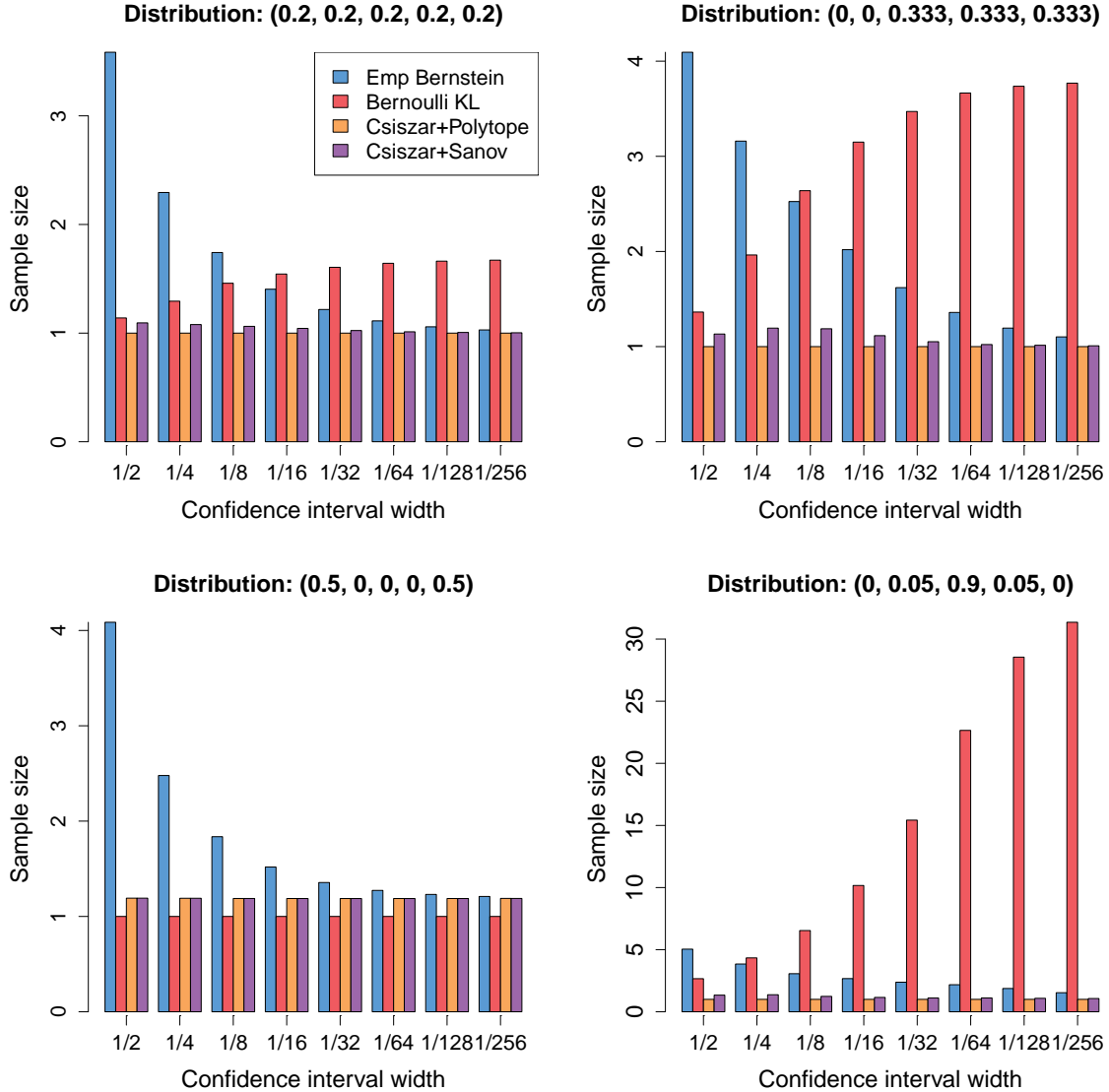


Figure 5: Average sample size requirements as a function of confidence interval width (20 repetitions at each sample size / interval width). The required sample sizes are very stable (essentially constant) over repetitions. Sample sizes are normalized to the smallest/best (among the various methods) at each width. The empirical Bernstein bound (blue) typically requires several times more samples than our new bounds (orange and purple) at small sample sizes (large interval widths), but eventually improves as the sample sizes increase, as expected. The Bernoulli-KL bound (red) performs comparatively well at small sample sizes, but generally degrades at larger sample size (smaller interval widths), sometimes requiring several times more samples than our new bounds. The third distribution (1/2, 0, 0, 0, 1/2) is an exceptional case, since it corresponds to a Bernoulli distribution and the Bernoulli-KL bound is ideal for such cases.

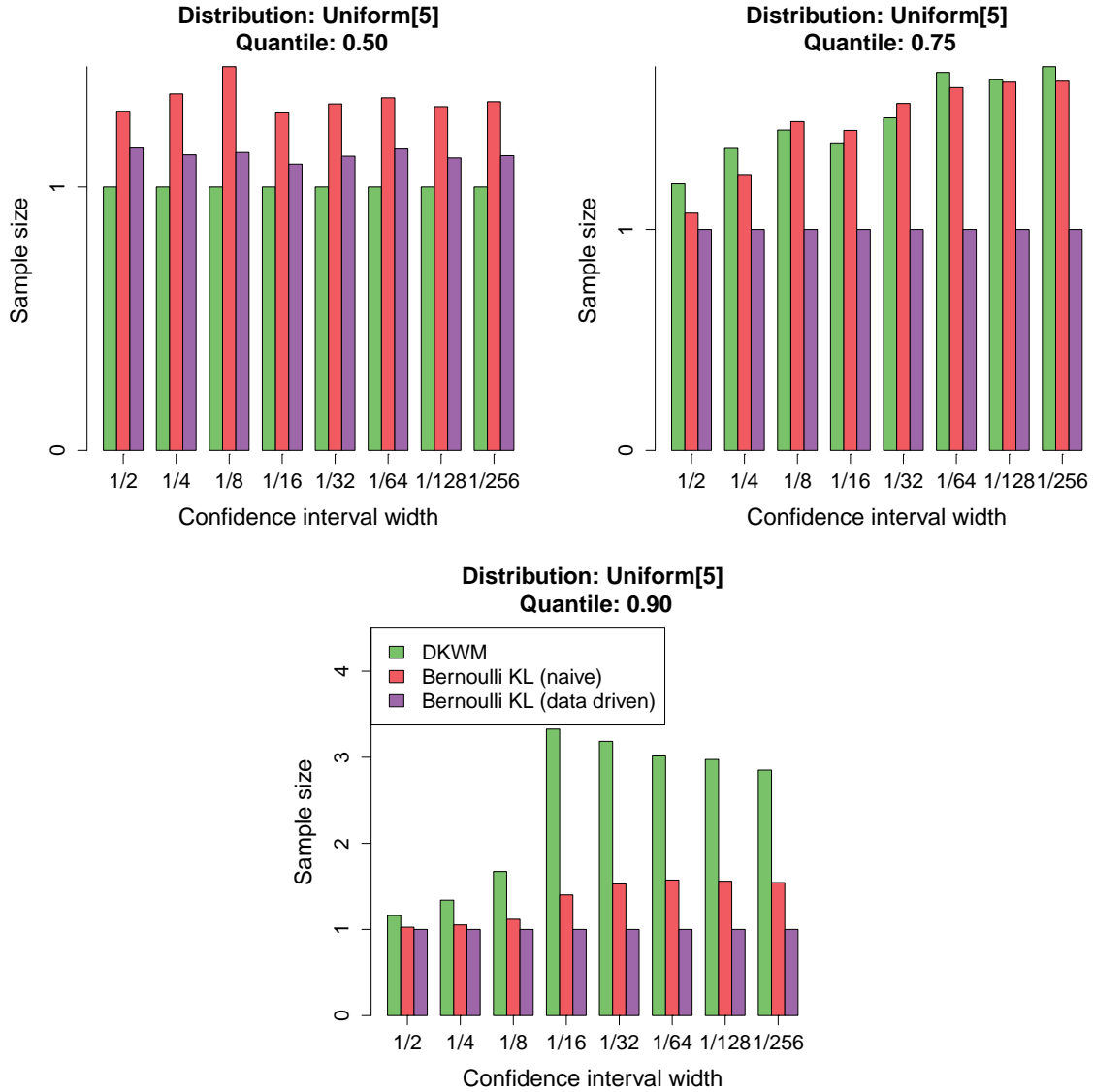


Figure 6: Average sample size needed for the width of the confidence interval for the quantile to reach a desired level based on 20 repetitions, for various quantiles. The required sample sizes are very stable (essentially constant) over repetitions. Sample sizes are normalized to the best (among the methods) at each width. The new Bernoulli-KL CDF bounds perform significantly better than the DKWM bound for more extreme quantiles like 0.9.

References

- [1] ADOMAVICIUS, G., KAMIREDDY, S., AND KWON, Y. Towards more confident recommendations: Improving recommender systems using filtering approach based on rating variance. In *Proc. of the 17th Workshop on Information Technology and Systems* (2007), pp. 152–157.
- [2] AUDIBERT, J.-Y., MUNOS, R., AND SZEPESVÁRI, C. Exploration–exploitation tradeoff using variance estimates in multi-armed bandits. *Theoretical Computer Science* 410, 19 (2009), 1876–1902.
- [3] BALSUBRAMANI, A., AND RAMDAS, A. Sequential nonparametric testing with the law of the iterated logarithm. In *Proceedings of the Thirty-Second Conference on Uncertainty in Artificial Intelligence* (2016), AUAI Press, pp. 42–51.
- [4] BOUCHERON, S., LUGOSI, G., AND MASSART, P. *Concentration inequalities: A nonasymptotic theory of independence*. Oxford university press, 2013.
- [5] BOYSEN, G. A. Uses and misuses of student evaluations of teaching: The interpretation of differences in teaching evaluation means irrespective of statistical information. *Teaching of Psychology* 42, 2 (2015), 109–118.
- [6] COHEN, P. A. Student ratings of instruction and student achievement: A meta-analysis of multi-section validity studies. *Review of educational Research* 51, 3 (1981), 281–309.
- [7] COVER, T. M., AND THOMAS, J. A. *Elements of information theory*. John Wiley & Sons, 2012.
- [8] CSISZÁR, I. Sanov property, generalized i-projection and a conditional limit theorem. *The Annals of Probability* (1984), 768–793.
- [9] DUEMBGEN, L., AND WELLNER, J. A. Confidence bands for distribution functions: A new look at the law of the iterated logarithm. *arXiv preprint arXiv:1402.2918* (2014).
- [10] GARIVIER, A., AND CAPPÉ, O. The kl-ucb algorithm for bounded stochastic bandits and beyond. In *Proceedings of the 24th annual Conference On Learning Theory* (2011), pp. 359–376.
- [11] KWON, Y. Improving top-n recommendation techniques using rating variance. In *Proceedings of the 2008 ACM conference on Recommender systems* (2008), ACM, pp. 307–310.
- [12] MARDIA, J., JIAO, J., TÁNCZOS, E., NOWAK, R. D., AND WEISSMAN, T. Concentration inequalities for the empirical distribution. *arXiv preprint arXiv:1809.06522* (2018).
- [13] MASSART, P. The tight constant in the dvoretzky-kiefer-wolfowitz inequality. *The annals of Probability* (1990), 1269–1283.
- [14] MAURER, A., AND PONTIL, M. Empirical bernstein bounds and sample variance penalization. *arXiv preprint arXiv:0907.3740* (2009).
- [15] MNIH, V., SZEPESVÁRI, C., AND AUDIBERT, J.-Y. Empirical bernstein stopping. In *Proceedings of the 25th international conference on Machine learning* (2008), ACM, pp. 672–679.
- [16] PEEL, T., ANTHOINE, S., AND RALAIVOLA, L. Empirical bernstein inequalities for u-statistics. In *Advances in Neural Information Processing Systems* (2010), pp. 1903–1911.
- [17] SANOV, I. N. On the probability of large deviations of random variables. Tech. rep., North Carolina State University. Dept. of Statistics, 1958.
- [18] SZORENYI, B., BUSA-FEKETE, R., WENG, P., AND HÜLLERMEIER, E. Qualitative multi-armed bandits: A quantile-based approach. In *32nd International Conference on Machine Learning* (2015), pp. 1660–1668.
- [19] TÁNCZOS, E., NOWAK, R., AND MANKOFF, B. A kl-lucb algorithm for large-scale crowdsourcing. In *Advances in Neural Information Processing Systems* (2017), pp. 5894–5903.

A Running shoe example

The shoes and the ratings in the example of Section 1 are Shoe 1 and Shoe 2.

B Proof of Theorem 3

We begin with setting up notation. Without loss of generality, assume that X takes values from $[k]$. For any n -length sequence $x \in [k]^n$, let T_x denote the *type* of x (the empirical distribution generated by the sequence). Denote the set of all types based on n -length sequences by \mathcal{T}_n , formally $\mathcal{T}_n = \{T_x : x \in [k]^n\}$. We use the shorthand notation $\mathbb{P}(E) = \mathbb{P}(x : T_x \in E)$.

Define the distribution $\bar{\mathbb{P}}(i) = \sum_{x \in [k]^n} \mathbb{Q}(x) T_x(i)$, where \mathbb{Q} is an arbitrary distribution over n -length sequences. Then

$$\begin{aligned} \mathbb{P}(E) &= \exp(\log \mathbb{P}(E)) \\ &= \exp\left(\sum_{x \in [k]^n} \mathbb{Q}(x) \log \mathbb{P}(E)\right) \\ &= \exp\left(\sum_{x \in [k]^n} \mathbb{Q}(x) \log \frac{\mathbb{P}(x)}{\bar{\mathbb{P}}(x)}\right. \\ &\quad \left.+ \sum_{x \in [k]^n} \mathbb{Q}(x) \log \frac{\bar{\mathbb{P}}(x) \mathbb{P}(E)}{\mathbb{P}(x)}\right). \end{aligned}$$

But

$$\begin{aligned} &\sum_{x \in [k]^n} \mathbb{Q}(x) \log \frac{\mathbb{P}(x)}{\bar{\mathbb{P}}(x)} \\ &= \sum_{x \in [k]^n} \mathbb{Q}(x) \log \prod_{j \in [k]} \left(\frac{\mathbb{P}(j)}{\bar{\mathbb{P}}(j)}\right)^{n T_x(j)} \\ &= \sum_{x \in [k]^n} \mathbb{Q}(x) t \sum_{j \in [k]} T_x(j) \log \frac{\mathbb{P}(j)}{\bar{\mathbb{P}}(j)} \\ &= -n \text{KL}(\bar{\mathbb{P}}, \mathbb{P}), \end{aligned}$$

so

$$\begin{aligned} \mathbb{P}(E) &= \exp\left(-n \text{KL}(\bar{\mathbb{P}}, \mathbb{P})\right. \\ &\quad \left.+ \sum_{x \in [k]^n} \mathbb{Q}(x) \log \frac{\bar{\mathbb{P}}(x) \mathbb{P}(E)}{\mathbb{P}(x)}\right). \end{aligned} \tag{7}$$

Now we use a specific choice for \mathbb{Q} . Let $\mathbb{Q}(x) = \mathbf{1}\{x \in E\} \mathbb{P}(x) / \mathbb{P}(E) := P_E(x)$ for short. Then

$$\sum_{x \in [k]^n} \mathbb{Q}(x) \log \frac{\bar{\mathbb{P}}(x) \mathbb{P}(E)}{\mathbb{P}(x)} = -\text{KL}(\mathbb{P}_E, \bar{\mathbb{P}}),$$

and so

$$\mathbb{P}(E) \leq \exp(-n \text{KL}(\bar{\mathbb{P}}, \mathbb{P})).$$

If E is convex and \mathbb{Q} is supported on E (note that with the above choice this is true), then $\bar{\mathbb{P}} \in E$ and hence

$$\mathbb{P}(E) \leq \exp\left(-n \inf_{\mathbb{P}' \in E} \text{KL}(\mathbb{P}', \mathbb{P})\right).$$

C Proof of Proposition 3

We begin by providing the road map for the proof. The high-level argument is that when ϵ is small, the minimizer of $\min_{\mathbb{Q} \in E} \text{KL}(\mathbb{Q}, \mathbb{P})$ will be close to \mathbb{P} . When \mathbb{P} and \mathbb{Q} are close, $\text{KL}(\mathbb{Q}, \mathbb{P}) \approx \chi^2(\mathbb{Q}, \mathbb{P})$. Minimizing the chi-squared divergence instead of the KL-divergence on E would precisely give the value $\epsilon^2/(2 \text{Var}_{\mathbb{P}}(\mathcal{F}))$.

Carrying out the proof formally requires care, in particular to be able to switch between $\min_{\mathbb{Q} \in E} \text{KL}(\mathbb{Q}, \mathbb{P})$ and $\min_{\mathbb{Q} \in E} \chi^2(\mathbb{Q}, \mathbb{P})$.

We begin by upper bounding the order of magnitude of $\min_{\mathbb{Q} \in E} \text{KL}(\mathbb{Q}, \mathbb{P})$ in terms of ϵ . This will be necessary to control the error we induce by switching between the two optimizations.

Let $\mathbb{Q}' \in E$ be such that $q'_i/p_i = \lambda w_i + \nu$ with some $\lambda, \nu > 0$. Note that in order for \mathbb{Q}' to be a proper distribution we must have

$$1 = \sum_{i \in [k]} p_i (\lambda w_i + \nu) = \lambda \mathcal{F}(\mathbb{P}) + \nu. \quad (8)$$

In order for \mathbb{Q}' to be in E we need

$$\begin{aligned} \epsilon &= \sum_{i \in [k]} (q'_i - p_i) w_i \\ &= \sum_{i \in [k]} p_i w_i (\lambda w_i + \nu - 1) \\ &= \lambda \sum_{i \in [k]} p_i w_i (w_i - \mathcal{F}(\mathbb{P})) \\ &= \lambda \text{Var}_{\mathbb{P}}(\mathcal{F}), \end{aligned} \quad (9)$$

where in the third line we used (8).

From (8) and (9) we can conclude that

$$\begin{aligned} q'_i/p_i &= \lambda w_i + 1 - \mathcal{F}(\mathbb{P}) \\ &= 1 + \frac{\epsilon}{\text{Var}_{\mathbb{P}}(\mathcal{F})} (\mathcal{F}(\mathbb{P}) - w_i) \\ &= 1 + O(\epsilon), \end{aligned}$$

for all $i \in [k]$.

Note that clearly $\min_{\mathbb{Q} \in E} \text{KL}(\mathbb{Q}, \mathbb{P}) \leq \text{KL}(\mathbb{Q}', \mathbb{P})$. We will upper bound the right hand side when ϵ is small. In particular, we will use the Taylor expansion of $x \log x$ around $x = 1$ with a Lagrange remainder term, i.e.

$$x \log x = (x - 1) + \frac{1}{2}(x - 1)^2 - \frac{1}{6\xi^2}(x - 1)^3,$$

where $\xi \in (1 - a, 1 + a)$ and a is the radius of the expansion. Since we concluded that q'_i/p_i is close to 1, we can choose a to be some arbitrary constant when ϵ is small enough.

Using the Taylor expansion above, and the fact that $q'_i/p_i \in (1 - O(\epsilon), 1 + O(\epsilon))$ we get that

$$\begin{aligned} \text{KL}(\mathbb{Q}', \mathbb{P}) &= \sum_{i \in [k]} p_i \frac{q'_i}{p_i} \log \frac{q'_i}{p_i} \\ &= \sum_{i \in [k]} p_i \left(\left(\frac{q'_i}{p_i} - 1 \right) + \frac{1}{2} \left(\frac{q'_i}{p_i} - 1 \right)^2 \right. \\ &\quad \left. - \frac{1}{6\xi_i^2} \left(\frac{q'_i}{p_i} - 1 \right)^3 \right) \\ &\leq \frac{1}{2} \sum_{i \in [k]} \left(\frac{q'_i}{p_i} - 1 \right)^2 + O(\epsilon^3) \\ &\leq \frac{1}{2} \left(\sum_{i \in [k]} \frac{q_i'^2}{p_i} - 1 \right) + O(\epsilon^3). \end{aligned}$$

Plugging in $q'_i/p_i = \lambda w_i + \nu$ and using (8) and (9) we can continue as

$$\begin{aligned}
\text{KL}(\mathbb{Q}', \mathbb{P}) &\leq \frac{1}{2} \left(\sum_{i \in [k]} \frac{q_i'^2}{p_i} - 1 \right) + O(\epsilon^3) \\
&= \frac{1}{2} \left(\sum_{i \in [k]} q_i' \lambda w_i + \nu - 1 \right) + O(\epsilon^3) \\
&= \frac{1}{2} \lambda \sum_{i \in [k]} q_i' (w_i - \mathcal{F}(\mathbb{P})) + O(\epsilon^3) \\
&= \frac{\epsilon^2}{2 \text{Var}_{\mathbb{P}}(\mathcal{F})} + O(\epsilon^3) .
\end{aligned}$$

So far we have shown that $\min_{\mathbb{Q} \in E} \text{KL}(\mathbb{Q}, \mathbb{P}) \leq \epsilon^2 / (2 \text{Var}_{\mathbb{P}}(\mathcal{F})) + O(\epsilon^3)$. We now use this to switch from the optimization of the KL-divergence to that of the χ^2 -distance.

First we use the upper bound above to conclude that the unique minimizer⁹ to $\min_{\mathbb{Q} \in E} \text{KL}(\mathbb{Q}, \mathbb{P})$ denoted by \mathbb{Q}^* is also close to \mathbb{P} in Total-Variation distance. This fact is a simple consequence of Pinsker's inequality:

$$\text{TV}(\mathbb{Q}^*, \mathbb{P}) \leq \sqrt{\text{KL}(\mathbb{Q}^*, \mathbb{P})/2} = O(\epsilon) ,$$

where $\text{TV}(\cdot, \cdot)$ denotes the Total Variation distance, and on the right side we used $\text{KL}(\mathbb{Q}^*, \mathbb{P}) \leq O(\epsilon^2)$. Denoting the Total Variation ball of radius z around \mathbb{P} by $B_{\text{TV}}(\mathbb{P}, z)$ we have now shown that $\mathbb{Q}^* \in B_{\text{TV}}(\mathbb{P}, O(\epsilon))$.

We are finally in position to formally show the lower bound for $\min_{\mathbb{Q} \in E} \text{KL}(\mathbb{Q}, \mathbb{P})$. In particular

$$\begin{aligned}
\min_{\mathbb{Q} \in E} \text{KL}(\mathbb{Q}, \mathbb{P}) &= \min_{\mathbb{Q} \in E \cap B_{\text{TV}}(\mathbb{P}, O(\epsilon))} \text{KL}(\mathbb{Q}, \mathbb{P}) \\
&= \min_{\mathbb{Q} \in E \cap B_{\text{TV}}(\mathbb{P}, O(\epsilon))} \left(\frac{1}{2} \left(\sum_{i \in [k]} \frac{q_i^2}{p_i} - 1 \right) \right. \\
&\quad \left. - \frac{1}{6\xi(q_i, p_i)^2} \left(\frac{q_i}{p_i} - 1 \right)^3 \right) ,
\end{aligned}$$

using the same Taylor-expansion as before. Note that the Taylor expansion is valid here because we are only considering distributions \mathbb{Q} that are close to \mathbb{P} , i.e. $\mathbb{Q} \in E \cap B_{\text{TV}}(\mathbb{P}, O(\epsilon))$.

However, for distributions \mathbb{Q} in $B_{\text{TV}}(\mathbb{P}, O(\epsilon))$ we have $q_i/p_i - 1 = O(\epsilon)$. Hence we can continue as

$$\begin{aligned}
&\min_{\mathbb{Q} \in E} \text{KL}(\mathbb{Q}, \mathbb{P}) \\
&= \min_{\mathbb{Q} \in E \cap B_{\text{TV}}(\mathbb{P}, O(\epsilon))} \left(\frac{1}{2} \left(\sum_{i \in [k]} \frac{q_i^2}{p_i} - 1 \right) \right. \\
&\quad \left. - \frac{1}{6\xi(q_i, p_i)^2} \left(\frac{q_i}{p_i} - 1 \right)^3 \right) \\
&\geq \min_{\mathbb{Q} \in E \cap B_{\text{TV}}(\mathbb{P}, O(\epsilon))} \frac{1}{2} \left(\sum_{i \in [k]} \frac{q_i^2}{p_i} - 1 \right) - O(\epsilon^3) \\
&\geq \min_{\mathbb{Q} \in E} \frac{1}{2} \left(\sum_{i \in [k]} \frac{q_i^2}{p_i} - 1 \right) - O(\epsilon^3) .
\end{aligned}$$

All that is left to do is to solve the optimization of the χ^2 -divergence. In detail, the optimization we

⁹We know that \mathbb{Q}^* is unique since E is convex.

need to solve is

$$\begin{aligned} \min \frac{1}{2} \left(\sum_{j \in [k]} \frac{q_j^2}{p_j} - 1 \right) \text{ s.t.} \\ \sum_{j \in [k]} q_j = 1, \quad q_j \geq 0, \quad \forall j \in [k], \\ \sum_{j \in [k]} w_j (q_j - p_j) = \epsilon. \end{aligned}$$

Taking the derivative of Lagrangian w.r.t. q_j yields

$$\frac{\partial}{\partial q_j} \mathcal{L}(\underline{q}, \lambda, \nu, \underline{\eta}) = \frac{q_j}{p_j} - \lambda w_j - \nu - \eta_j.$$

Equating this to zero and rearranging gives an expression for the optimizer \mathbb{Q} .

Without loss of generality, we can assume that \mathbb{P} is in the interior of the simplex, since otherwise we would just restate the entire argument in lower dimension. If ϵ is small enough then the optimizer will satisfy $q_j > 0 \forall j \in [k]$ ¹⁰. Thus the KKT optimality conditions give $\eta_j = 0$ for all $j \in [k]$. Hence we have that the solution of the optimization \mathbb{Q}^* satisfies

$$\frac{q_j^*}{p_j} = \lambda w_j + \nu.$$

From this point on we continue the same way as we did at the beginning of the proof to finally conclude

$$\min_{\mathbb{Q} \in E} \text{KL}(\mathbb{Q}, \mathbb{P}) \geq \frac{\epsilon^2}{2 \text{Var}_{\mathbb{P}}(\mathcal{F})} - O(\epsilon^3).$$

D Figures for numerical experiments

D.1 Linear Functionals

We present the plots corresponding to the numerical experiments that we omitted from the main body of the paper. The plots shown here correspond to experiments with various values of the true distribution. Regardless, all experiments tell a similar story to the one outlined in the paper.

D.2 Quantiles

The larger the alphabet size k , potentially the bigger problem the union bound becomes when using the KL-Bernoulli CDF bounds. We present similar numerical experiments to those in the main body of the paper, but for $k = 10$. The results tell a similar story: the performance of the KL-based bounds is not much worse than the DKWM near the median, but get much better for quantiles far from the median.

¹⁰We omit a detailed argument here, but this is clear: the optimization problem considered here is searching for an ellipse centered at \mathbb{P} that touches the half-space E .

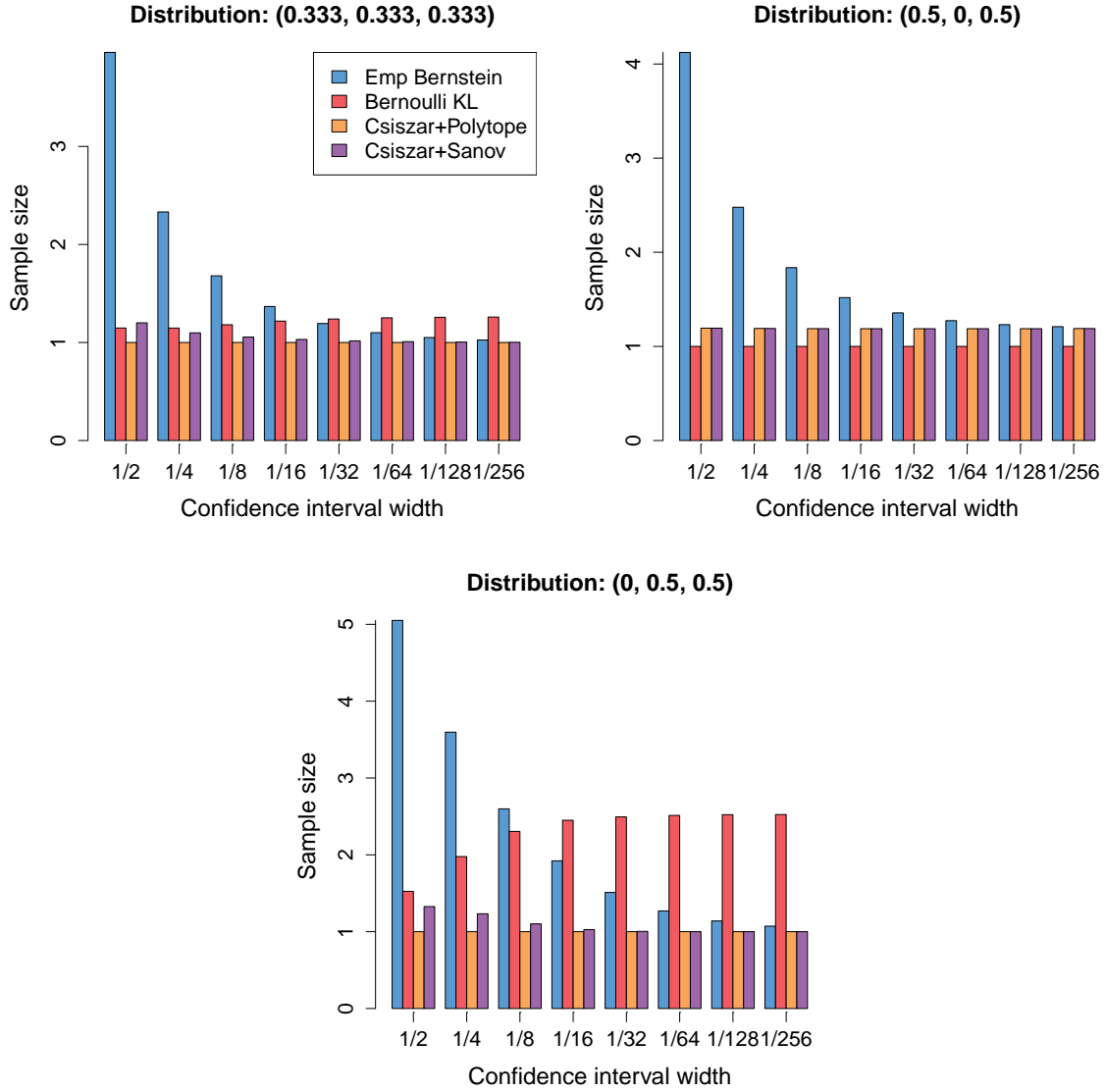


Figure 7: Average sample size needed for the width of the confidence bound for the mean to reach a desired level, for various distributions. The high-level findings are similar for all cases: Empirical Bernstein (blue) performs poorly in the small sample regime (large interval width), but improves as the sample size increases. Bernoulli-KL (red) performs relatively well for small samples, but its performance deteriorates, unless the true distribution is Bernoulli, in which case it performs best. Our new bounds (orange and purple) perform best uniformly across all sample sizes, and have comparable performance to the Bernoulli-KL when the distribution is Bernoulli.

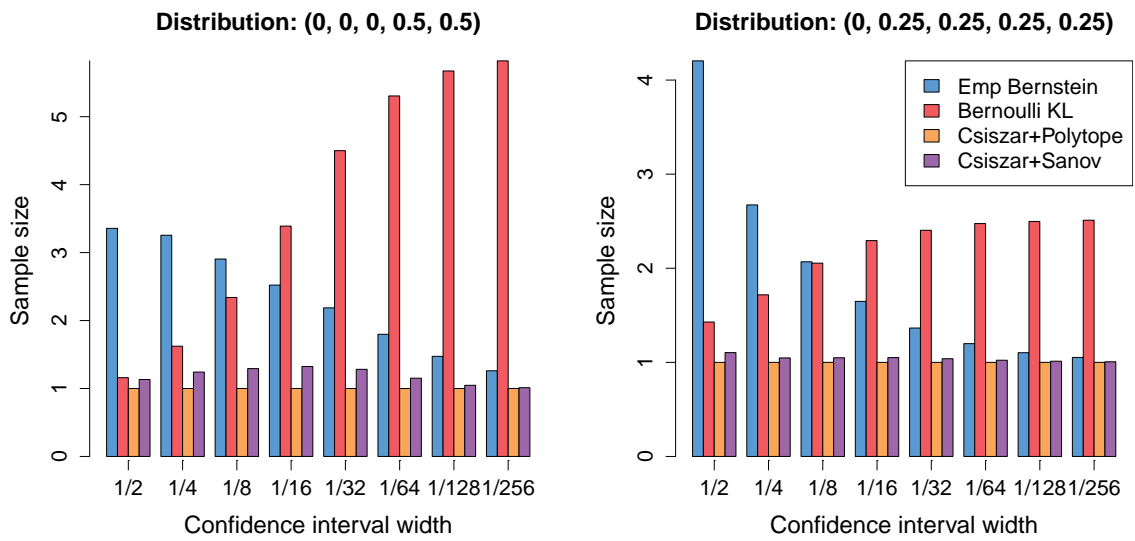


Figure 8: Average sample size needed for the width of the confidence bound for the mean to reach a desired level, for various distributions. The high-level findings are similar for all cases: Empirical Bernstein (blue) performs poorly in the small sample regime (large interval width), but improves as the sample size increases. Bernoulli-KL (red) performs relatively well for small samples, but its performance deteriorates, unless the true distribution is Bernoulli, in which case it performs best. Our new bounds (orange and purple) perform best uniformly across all sample sizes, and have comparable performance to the Bernoulli-KL when the distribution is Bernoulli..

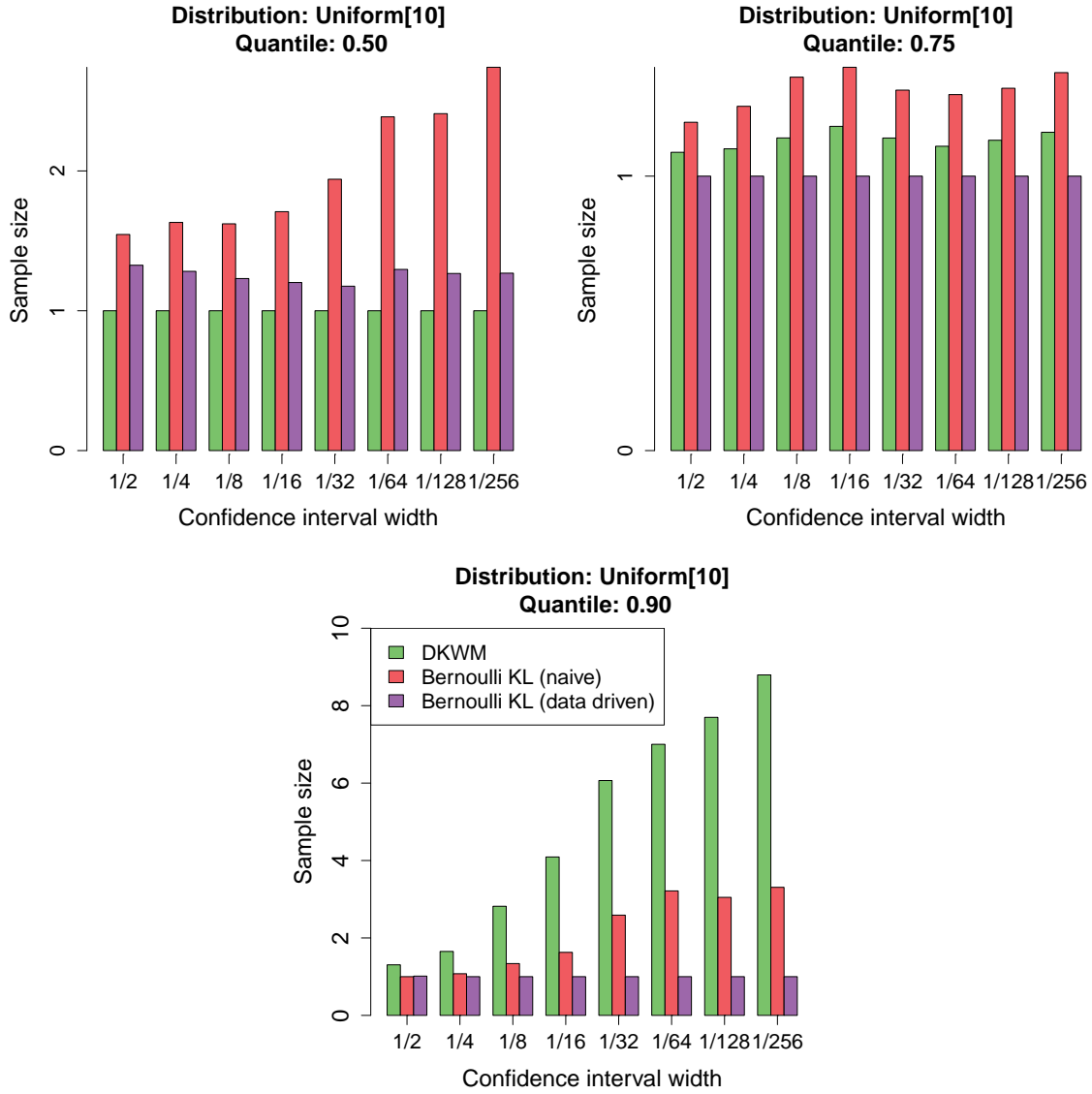


Figure 9: Average sample size needed for the width of the confidence bound for the quantile to reach a desired level, for various quantiles. The true distribution is Unif[10] in all cases. The Bernoulli-KL bound with a data-driven union bound (purple) shows better performance compared to the one with a naive union bound (red) across the board. The figures indicate comparable performance between the DKWM bound (green) and the Bernoulli-KL bound with a data-driven union bound (purple) for quantiles around the median. However, for the 90% quantile, the Bernoulli KL bounds clearly outperform the DKWM bounds.